Low-Frequency Dielectric Investigations into the Phase Behavior of Glyceryl Monoolein/Water Systems

Renren He and Duncan Q. M. Craig*

Centre for Material Science, School of Pharmacy, University of London, 29-39 Brunswick Square, London WC1N 1AX, U.K.

Received: July 23, 1997; In Final Form: November 14, 1997

A series of glyceryl monoolein/water liquid crystal systems containing 15%, 20%, 30%, and 35% w/w water have been investigated using dielectric spectroscopy over a frequency range of $10^{-3}-10^{6}$ Hz and a temperature range of 20−90 °C in order to facilitate association of the lyotropic and thermotropic phase behavior with the dielectric response. The phase boundaries of the mixes were determined independently using hot stage microscopy. The frequency-dependent dielectric spectra of systems containing lamellar, cubic, and hexagonal phases are reported and have been modeled using circuits corresponding to generalized Maxwell−Wagner responses. More specifically, the systems were found to correspond to a parallel bulk capacitance and conductance in series with a Maxwell−Wagner blocking capacitance, which was associated with an adsorbed layer at the electrode surfaces. An additional dispersion was observed corresponding to a series *RC* circuit, which was associated with charge transport across the lipid bilayers. It is proposed that the dielectric responses of the lamellar, cubic, and hexagonal phases exhibited by these systems may be described in terms of equivalent circuit models, which may in turn be related to specific structural features of the sample.

Introduction

Dielectric analysis involves the application of an oscillating electrical field to a sample and the subsequent measurement of the real and imaginary components of the response over a range of frequencies ω. This response may be expressed in terms of the complex permittivity $\epsilon^*(\omega)$, where

$$\epsilon^*(\omega) = \epsilon'(\omega) - i\epsilon''(\omega) \tag{1}$$

with ϵ' and ϵ'' being the real and imaginary components at frequency ω and i being the square root of -1. These components may be measured in terms of the extrinsic parameters $C(\omega)$ and $G(\omega)/\omega$, where $C(\omega)$ is the capacitance and $G(\omega)/\omega$ is the dielectric loss, $G(\omega)$ being the conductance (representing the sum of the ac and dc contributions). The relationship between the real permittivity and the capacitance is given by

$$\epsilon'(\omega) = \frac{C(\omega)d}{A\epsilon_0} \tag{2}$$

where ϵ_0 is the permittivity of free space and d and A are the interelectrode distance and electrode area, respectively. Similarly, the imaginary permittivity is related to the dielectric loss via

$$\epsilon''(\omega) = \frac{G(\omega)}{\omega}\frac{d}{A\epsilon_0} \tag{3}$$

While this method has been widely used as a means of characterizing the electrical properties of materials, it is also possible to relate those properties to specific structural features of the sample. The possibility of using the method as a means of characterizing the physical structures of complex materials has led to recent diversification of recognized applications for the approach into fields such as the pharmaceutical sciences.[1] To develop dielectric analysis within such applied disciplines, it is essential to clarify the relationship between the electrical and structural properties of materials, particularly for condensed systems for which non-Debye behavior is almost universal. Jonscher[2] has suggested that the deviation from ideality (and in particular power law relationships between permittivity and frequency) is due to many-body interactions between dipolar species. Dissado and Hill[3] developed a quantum mechanical approach based on the premise of samples being composed of clusters of dipoles that show cooperativity both within and between clusters. The nonideal behavior observed experimentally can be described by power law exponents that relate to the degree of cooperativity between dipoles; hence the approach allows interpretation of the dielectric data using parameters with specific structural meaning.

The approach has also been developed by Hill and Pickup[4] in the context of the low-frequency (kHz to sub-Hz) behavior of heterogeneous liquid systems, whereby the response is considered to be a combination of bulk-dominated and interface-dominated processes. In the kHz region the response is related to the polarization and charge-transfer processes within the bulk of the sample, whereas at lower (sub-Hz) frequencies, the response is dominated by barrier layers formed by adsorbed molecules of the sample components at the electrode surfaces. Such behavior corresponds to a generalized Maxwell−Wagner system,[4] which may be modeled by a series connection of two parallel *RC* circuits. For a dispersive system, the equivalent elements are frequency-dependent and may be described using power law exponents, e.g. $C(\omega) \propto (i\omega)^{-s}$ with s positive and less than unity. This approach has been used to interpret the low-frequency responses of a number of liquid and semisolid systems, particularly by the group of Hill[4−9] and our group.[10−14]

* Corresponding author. tel/fax: (44) 171 753 5863. e mail: duncraig@ulsop.ac.uk.

S1089-5647(97)02388-2 CCC: $15.00
Published on Web 02/18/1998

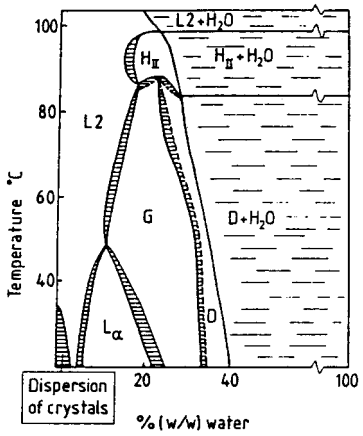

Figure 1. Phase diagram of monoolein/water, adapted from ref 15, showing the L_2, L_α, H_{11}, and cubic phases in relation to temperature and water content. The bicontinuous cubic phases are denoted G and D.

To provide a basis for understanding the relationship between the electrical and structural properties of semisolids, glyceryl monoolein/water mixes have been studied, as these materials form well-defined liquid crystalline phases depending on temperature and solvent concentration, as shown in Figure 1.[15] In addition, these materials have been investigated as potential drug delivery systems.[16−18] Glyceryl monoolein is a water-insoluble swelling lipid; in the solid state the lipids exist as a stack of planar molecular bilayers containing closely packed hydrocarbon chains with the polar heads forming the outer surfaces. On addition of small quantities of water, reverse micelles (L_2) are formed. Depending on the water content and temperature, lamellar (L_α), cubic (C), and reversed hexagonal (H_{II}) forms are observed. The lamellar phase is a semifluid liquid crystalline system, consisting of lipid bilayers alternating with water layers which have long-range order in one dimension. The reversed hexagonal phase is periodic in two dimensions and consists of water cylinders separated by lipid bilayers. The cubic phase has a highly viscous and ordered bicontinuous structure with curved lipid bilayers separated by water channels and extending in three dimensions.[15] In addition, Larsson[15] has suggested the existence of two cubic-phase structures, denoted G and D, although the structural similarity of these phases is such that in practice the two are usually considered to be equivalent. It is therefore of interest to study the relationship between the phase behavior of these systems and the corresponding dielectric response, both in terms of developing low-frequency dielectric analysis in the study of liquid crystalline systems and also for investigating the possibility of using this approach as a means of identifying and characterizing the different liquid crystalline phases. The emphasis of this investigation is placed on exploring the potential of the low-frequency dielectric technique as a means of quantitatively characterizing these complex materials; in this particular case, a system that has already been studied using alternative techniques has been selected in order to allow verification of the conclusions drawn from the dielectric analysis. On this basis, therefore, it is possible to identify the features of the system that may be usefully characterized using the dielectric technique and to apply that knowledge to a range of other systems about which less is known.

Materials and Methods

A single batch of GMOrphic-80 glyceryl monoolein (Eastman Chemical Co.) was used throughout the study. This material is a distilled monoglyceride with a high monoolein content. All mixes were prepared using water with a resistivity of greater than 18 MΩ/cm, obtained from an ultrahigh-quality water purification system (Elga Co.). Four sets of gel sample containing 15%, 20%, 30%, and 35% w/w water were prepared. A known weight of GMOrphic-80 was gently heated to 60 °C, followed by the addition of water at the same temperature to produce the desired (% w/w) gel composition. The mix was stirred at 2000 rpm using a Heidolph RXR50 mixer. It was found that for samples containing 15% and 20% water uniform systems were obtained using 10−15 min of stirring, while for samples containing 30% and 35% water, a highly viscous gel was produced after only 10−15 s of high-speed mixing. Longer mixing times were found to produce no noticeable effect on the properties of the gels. The resulting sample was centrifuged at a speed of 3000 rpm for 20 min and then stored in a sealed container at room temperature for at least 24 h before use to allow equilibration of the samples.

While phase diagrams for glyceryl monooleate/water systems have been previously reported,[15−17] the basic material may show considerable variation between grades and batches; hence it was considered necessary to independently ascertain the phase behavior of the systems used here at the concentrations and temperatures under study by hot stage polarizing microscopy. The microscopic observations were performed using an Olympus differential interference contrast (DIC) microscope with Mettler hot stage facilities using a heating rate of 1 °C/min.

The dielectric measurements were carried out using a BDC-N broad band dielectric converter (Novocontrol GmbH) and a frequency response analyzer SI 1255 (Solatron-Schlumberger) linked to a Quatro temperature control system (Novocontrol GmbH). The sample was placed in a circular dielectric cell designed for liquid and semisolid samples with a diameter of 20 mm and an interelectrode distance of 0.5 mm. The frequency responses were obtained over a frequency range of 10^{-3}−10^{6} Hz with at least two measurement points taken at each frequency and each sample being reanalyzed at least once. The cell was cleaned thoroughly between measurements.

The fitting of the data was carried out by employing a modified generalized Maxwell−Wagner equivalent circuit with dispersive *RC* elements and using the Winfit 2.0 program supplied by Novocontrol GmbH. The main feature of Winfit 2.0 is nonlinear curve fitting of the measured data in the frequency domain, with both real and imaginary components being fitted simultaneously. In general impedance mode, the software supports up to four single fit terms which may hold several combinations of resistance, inductance, and capacitance elements and will also incorporate power law functions for these circuit features.

Results and Discussion

Establishment of Phase Behavior. By using a combination of microscopy and visual observation, the phase behavior at the four concentrations of GMOrphic-80 was established, thereby allowing identification of the phases present for each of the samples under study here. In all cases, the transition between the phases was seen over a narrow range of temperatures, as previously noted by Larsson.[15] The 15% w/w water systems were identified as being in the optically anisotropic lamellar (L_α) phase from ambient to 46 °C. Between 46 and 52 °C, the system gradually changed into the optically isotropic cubic phase. For the 20% systems the lamellar phase was observed from ambient to 44 °C and the cubic phase from 46 °C. The 30% systems were in the cubic phase from ambient

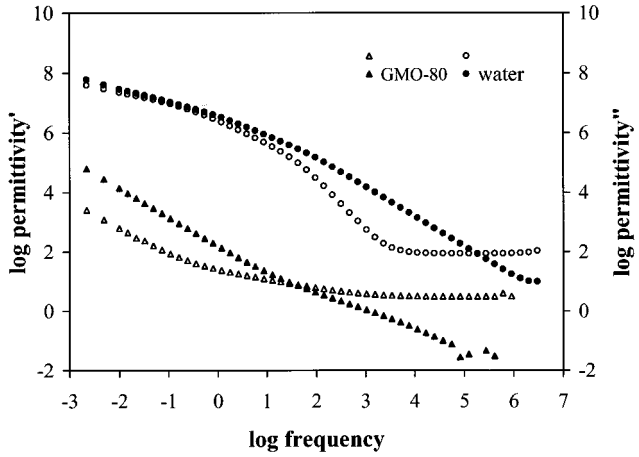

Figure 2. Low-frequency dielectric spectra for water and pure GMOrphic-80 at 23° C, showing the real and imaginary permittivities over the frequency range 10^{-2}—10^{5} Hz. Open symbols ϵ' (permittivity′); closed symbols ϵ'' (permittivity″).

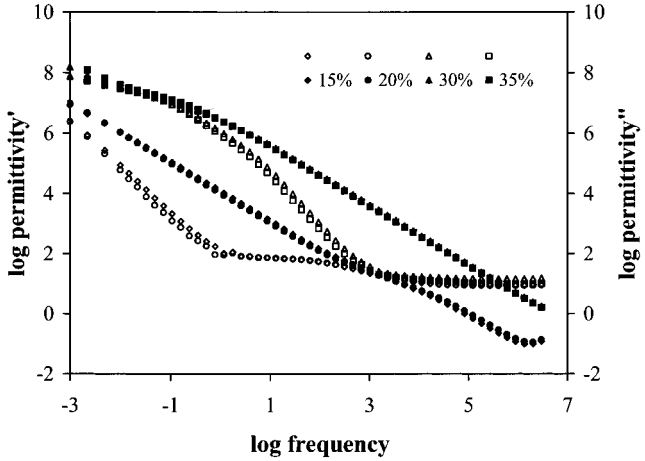

Figure 3. Low-frequency dielectric spectra of the GMOrphic-80/water systems with water contents of 15%, 20%, 30%, and 35% w/w at 23° C. Open symbols ϵ' (permittivity′); closed symbols ϵ'' (permittivity″).

to 61 °C and the reversed hexagonal phase above 68 °C; the latter was optically anisotropic and could be identified by angular or fanlike structures seen using polarizing microscopy. For the 35% systems, the cubic phase was observed from ambient to 62 °C, while the reversed hexagonal phase associated with a small proportion of free water was present above 69 °C. The boundaries identified are in reasonable agreement with the phase diagrams given previously.[15−17]

Dielectric Behavior of GMOrphic-80 and Water. The dielectric spectra for water and pure GMOrphic-80 are given in Figure 2, with the response expressed as the log real and imaginary permittivity against log frequency. The response for water may be described by a modification of the Maxwell−Wagner model, whereby the high-frequency (Hz to kHz) region is dominated by a bulk conductivity in parallel with a frequency-independent capacitance, while the low-frequency (sub-Hz) response is dominated by a diffusive electrode barrier layer, possibly corresponding to the presence of residual dissolved ionic material, as described by Hill and Pickup.[4] The response of GMOrphic 80 alone shows a high-frequency (kHz) real permittivity with a value of approximately 3, reflecting the weakly polar nature of the material, in parallel with a loss component approximately 3 orders of magnitude lower than that of water, as one would expect for a lipophilic solid material.

Dielectric Behavior of the L_α and Cubic Phases. Figure 3 shows dielectric spectra of the samples with water contents of 15%, 20%, 30%, and 35% w/w at 23 °C, with the plots exhibiting clear differences between the responses of the lamellar and cubic structures. The cubic systems (30% and 35% w/w water) showed responses with greater magnitudes than the lamellar systems (15% and 20% water) by a factor of 1−2 orders of magnitude, depending on the frequency. In addition, a broad peak is seen for the real component for the lamellar-phase systems in the region of 10^2 Hz.

The spectra may be interpreted in terms of the generalized Maxwell−Wagner model. For the cubic systems (30% and 35% water), the dielectric response exhibited two principal processes. At higher frequencies (kHz to MHz) the spectra corresponded to the bulk response of the sample; a frequency-independent real permittivity value of approximately 10 was observed, together with an inverse frequency-dependent dielectric loss component, $\epsilon'' \propto (\omega)^{-1}$ over a frequency range of six decades from 1 to 10^6 Hz. As the frequency decreased to sub-Hz values, both the loss and the real components approached a common permittivity value (ca. 10^7), this value corresponding to a low-frequency dispersion caused by barrier layers on the electrodes.[4] The barrier layer may be represented by a frequency-dependent complex capacitance C_s given by

$$C_s = C_{s=0}(i\omega/\omega_s)^{-s} \tag{4}$$

where $C_{s=0}$ is the capacitance when $s = 0$ and ω_s is a characteristic frequency. The exponent s can be obtained from the slope of the real permittivity plot and was found to be 0.385 and 0.390 for the 30% and 35% systems, respectively. The large value of the permittivity (6 orders of magnitude greater than the bulk value) is an inverse function of the thickness of this surface layer, corresponding to a value of a few nanometers, indicating that this low-frequency response corresponds to an adsorbed layer present on the two electrode surfaces.

The dielectric response of the lamellar phase samples (15% and 20% w/w water) showed three dielectric processes. A high-frequency process, corresponding to the bulk response in the cubic-phase samples, was observed in the kHz region, with a frequency independent real permittivity value of approximately 8. The second process was indicated by a broad peak in the real component between frequencies 1 and 10^3 Hz; a slight dispersion from $\epsilon'' \propto (\omega)^{-1}$ was also seen in the imaginary component. Finally, the values of both the real and imaginary components increased in the sub-Hz frequency range, indicating the presence of electrode barrier layers, although for these systems the response of the layers could not be directly observed over the frequency range studied.

Thermotropic Transition of the L_α to Cubic Phase. The dielectric responses of the 15% w/w systems run at 30, 70, and 90 °C are shown in Figure 4. The response taken at 30 °C showed the expected lamellar spectrum with the three principle features discussed earlier, while at 70 °C both the real and imaginary components increased by approximately 2 orders of magnitude and the relaxation peak seen at approximately 10^3 Hz was no longer observed. Similarly, the crossover frequency shifted from approximately 4×10^3 Hz at 30 °C to 2×10^5 Hz at 70 °C. This frequency (ω_τ) represents the inverse bulk relaxation time ($1/\tau$) of the system, as by combining eq 2 and 3 for $\epsilon' = \epsilon''$,

$$\omega_\tau = \frac{G(\omega)}{C(\omega)} = \frac{1}{R(\omega)C(\omega)} = 1/\tau \tag{5}$$

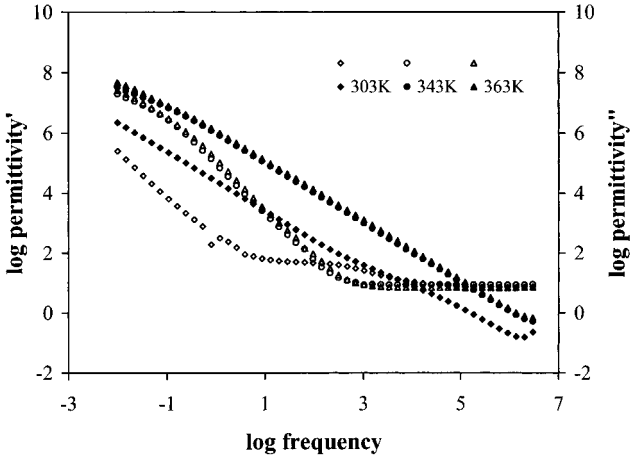

Figure 4. Low-frequency dielectric spectra of GMOrphic-80/water systems containing 15% w/w water obtained at 30°, 70°, and 90 °C. Open symbols ϵ' (permittivity′), closed symbols ϵ'' (permittivity″).

Hence the value of τ decreases on transition from the lamellar to the cubic phase by 2 orders of magnitude; this shift is conductance driven, reflecting the change in the imaginary component of the response on altering phases. The phase transition from the L_α to cubic phase at approximately 50 °C is therefore clearly reflected by the changes in spectral shape and magnitude, which correspond to the lyotropic phase changes noted in Figure 3. Furthermore, the changes in the response with temperature within a single phase were considerably smaller, as demonstrated by the similarity between the 70 and 90 °C systems.

Thermotropic Transition of the Cubic to H_{II} Phase. The dielectric responses of the 30% w/w samples are shown in Figure 5a. At 30 °C, the spectra exhibited features typical of the reponse corresponding to the cubic structure, as discussed above. However, on heating to 70 and 90 °C, both the real and imaginary components of the permittivity were reduced by a factor between approximately 2 and 10, depending on the frequency. Similarly, the bulk crossover frequency shifted from 3×10^5 Hz at 30 °C to 1.5×10^5 Hz at 70 °C, indicating a doubling of the bulk relaxation time. These alterations correspond to the change from the cubic to the reverse hexagonal phase at approximately 65 °C noted using hot stage microscopy, implying that the change from three- to two-dimensional periodicity on increasing the temperature may alter the tortuosity of the charge conduction pathway. It was also noted that the samples corresponding to the hexagonal phase showed the presence of a peak in the real permittivity and 10^4 Hz, as shown in Figure 5b. Similar trends were seen for the 35% system, although the changes in response seen on entering the reverse hexagonal phase were more pronounced (Figure 6).

Modeling of the Dielectric Response. As discussed above, the dielectric responses for all samples essentially corresponded to a bulk process at high frequencies (Hz to kHZ) and a dispersive Maxwell−Wagner barrier process at lower frequencies (sub-Hz). The low-frequency dielectric responses of the GMOrphic/water gel systems were therefore modeled by a modified generalized Maxwell−Wagner equivalent circuit, shown in Figure 7. This circuit consists of a fractional power law dispersive capacitance, C_s, representing a barrier at electrode surface, in series with a parallel *RC* circuit corresponding to the bulk processes. A bulk capacitance C_b in parallel with a bulk resistance R_b was used to model the principle bulk process, while the series *RC* element C_2R_2 represents a second relaxation process, with C_2 showing power law behavior described by

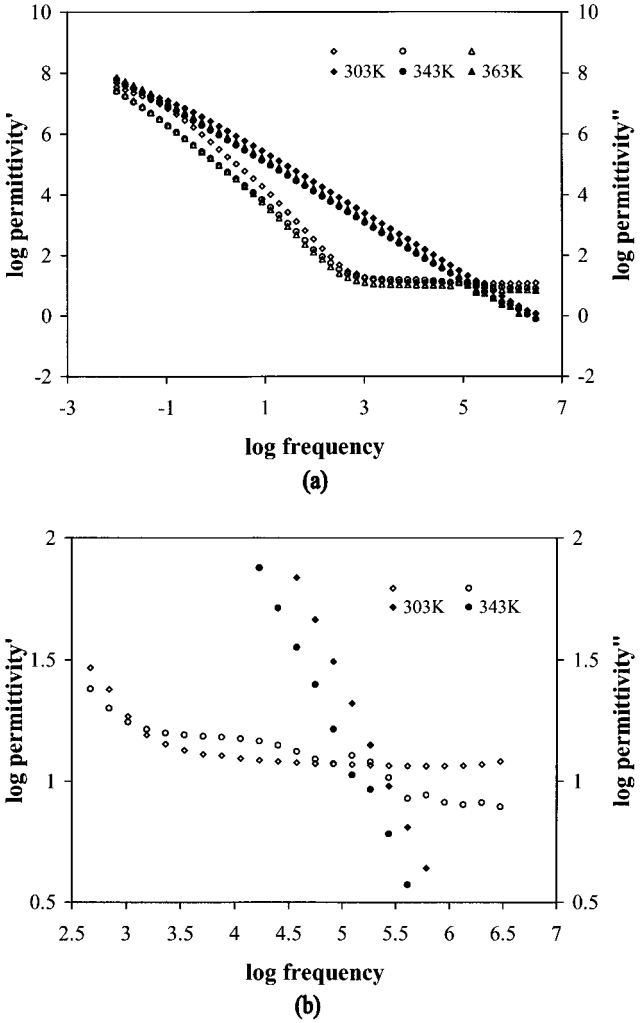

Figure 5. Low-frequency dielectric spectra of GMOrphic-80/water systems containing 30% w/w water (a) obtained at 30, 70, and 90 °C showing the response between 10^{-2} and 10^6 Hz and (b) obtained at 30 and 70 °C showing the response between 10^2 and 10^6 Hz. Open symbols ϵ' (permittivity′); closed symbols ϵ'' (permittivity″).

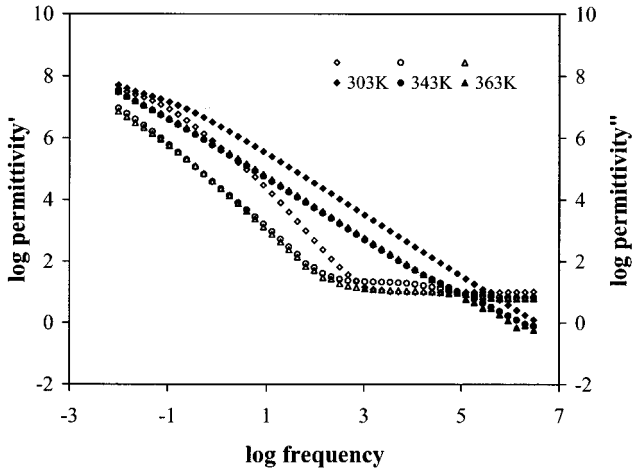

Figure 6. Low-frequency dielectric spectra of GMOrphic-80/water systems containing 35% w/w water obtained at 30, 70, and 90 °C. Open symbols ϵ' (permittivity′); closed symbols ϵ'' (permittivity″).

$$C_2 = C_{n=0}(i\omega/\omega_c)^{-n} = C_{n=0}(\omega/\omega_c)^{-n}[\cos(n\pi/2) - i\sin(n\pi/2)] \quad (6)$$

with $C_{n=0}$ and ω_c being characteristic capacitance and frequency values. The exponent n is related to the extent of cooperativity

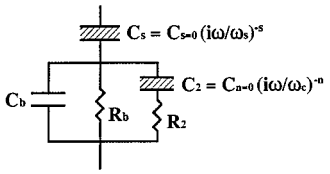

Figure 7. Modified generalized Maxwell−Wagner equivalent circuit employed to model the dielectric responses of the GMOrphic-80/water liquid crystal systems. See text for explanation of notation.

between the relaxing dipoles and the immediate environment and is therefore a reflection of the degree of ordering of the system.[4] When $n = 0$, C_2 is frequency-independent and the dipoles may be considered to be totally coupled to their surroundings, while when $0 < n < 1$, the dipoles are uncoupled and the value of $C_2(\omega)$ is complex and must be considered in terms of the real and imaginary components. Consequently, the circuit element is represented by a parallel RC circuit with $C_n \propto \omega^{-n}$ and $R_n \propto \omega^{n-1}$.

The model circuit shown in Figure 7 was found to give a satisfactory fit to all the experimental data. The values of the parameters obtained from the fitting data of the four concentrations are given in Table 1, while the fitting plots for the response of the 15% w/w water sample are shown in Figure 8 in conjunction with the experimental data as an example of the fitting correlation. The lamellar-phase behavior seen at 23 and 30 °C is reflected in the dielectric behavior by relatively high resistance values for both R_b and R_2 and markedly higher values for C_n and R_n than was seen for the cubic phase at higher temperatures. The values of C_n and R_n were also found to be frequency-dependent, as shown by the positive values of n, indicating relaxation and charge transport processes of weakly bound dipoles. The s value of approximately 0.5 indicates that the barrier layers at the electrode surfaces are diffusive in nature.[4] At higher temperatures, the value of C_2 was frequency independent and hence had no imaginary (resistance) component.

These fitted data may be considered in terms of the structure of the lamellar and cubic phases. The bulk response (C_b and R_b) reflects the gross behavior across the thickness of the sample, while the R_2C_2 series components represent further structural elements within that bulk, which may correspond to the lamellar network (or, more specifically, water dipoles within that network). Similar associations between circuit elements and lamellar structures have been proposed by Rowe et al.[6] for cetostearyl alcohol water systems. On increasing the temperature to 50 °C, the cubic phase was obtained for the 15% w/w systems and was characterized by a decrease in bulk resistance and nondispersive behavior for the R_2C_2 series element. This in turn reflects the isotropic bicontinuous structure of the cubic phase, leading to a decreased resistance and frequency independence due to the presence of continuous water channels within this phase.

The dielectric behavior of the 20% w/w systems showed a similar pattern on moving from the lamellar to the cubic phases. Similarly, the low-temperature (50 °C and below) values for the 30% and 35% systems were similar to the higher temperature values for the 15% and 20% mixes, as one would expect given the fact that both are cubic systems. On raising the temperature to form the hexagonal phase, an increase of approximately 1 order of magnitude or less was seen for the bulk resistance. However, an increase of 4 orders of magnitude in the value of R_2 was observed, again showing this circuit element to be highly sensitive to changes in phase. The structure of the hexagonal phase, comprising bilayers with a thickness of 4−5 nm surrounding water cylinders, may be expected to show a higher overall (bulk) resistance due to the discontinuity of charge transport in an anisotropic system compared to the isotropic cubic phase.

Conclusions

The data presented here indicate that low-frequency dielectric analysis is highly sensitive to the phase behavior of glyceryl monoolein water systems. Furthermore, the dielectric response may be effectively modeled by a comparatively simple circuit diagram, components of which may be related to specific features within the sample. In particular, the response of the electrode barrier layers may be modeled by a dispersive capacitor, thereby allowing their contribution to the total response to be identified. The bulk response may be modeled using a nondispersive parallel *RC* circuit, this element reflecting the overall electrical behavior through the thickness of the sample (discounting the electrode barrier layers). However, an additional series *RC* component, in parallel to the bulk response, has been included in the equivalent circuit. This component

TABLE 1: Values of the Fitted Equivalent Circuit Parameters Derived from the Experimental Data Obtained for GMOrphic-80/Water Systems Containing 15, 20, 30, and 35% w/w Water Using the Model Circuit Given in Figure 7

	T (°C)	R_b (Ω)	C_b (pF)	R_2 (Ω)	n	C_n at 1 kHz (pF)	R_n at 1 kHz (Ω)	s
15% water content	23	1.0×10^6	45.4	2.7×10^5	0.137	235.1	2.0×10^7	0.530
	30	1.3×10^6	43.2	2.7×10^5	0.110	211.9	2.7×10^7	0.524
	50	4.5×10^4	28.8	60.7	0.0	28.8		0.354
	70	2.8×10^4	22.2	70.2	0.0	28.0		0.339
	90	2.2×10^4	20.9	74.3	0.0	22.4		0.406
20% water content	23	1.3×10^6	45.6	3.0×10^5	0.123	192.6	2.7×10^7	0.519
	30	1.1×10^6	45.2	3.0×10^5	0.121	162.1	3.2×10^7	0.514
	40	5.4×10^4	49.8	2.6×10^5	0.09	68.1		0.376
	60	2.6×10^4	26.8	2.0	0.0	26.6		0.366
	80	2.1×10^4	21.3	75.4	0.0	27.1		0.376
	90	1.8×10^4	20.2	75.1	0.0	21.8		0.381
30% water content	23	1.1×10^4	31.2	90.0	0.0	44.9		0.385
	30	1.1×10^4	31.8	42.6	0.0	41.6		0.387
	50	6.0×10^3	27.7	11.3	0.0	29.8		0.408
	70	2.2×10^4	47.6	4.1×10^4	0.0	47.9		0.521
	90	1.9×10^4	39.3	4.6×10^4	0.0	16.4		0.504
35% water content	23	7.0×10^3	31.5	10.4	0.0	40.0		0.390
	30	8.3×10^3	30.1	11.1	0.0	32.8		0.369
	50	5.8×10^3	28.0	10.0	0.0	26.8		0.401
	70	5.6×10^4	35.4	3.1×10^4	0.0	68.7		0.571
	90	5.3×10^4	33.6	4.4×10^4	0.0	26.5		0.561

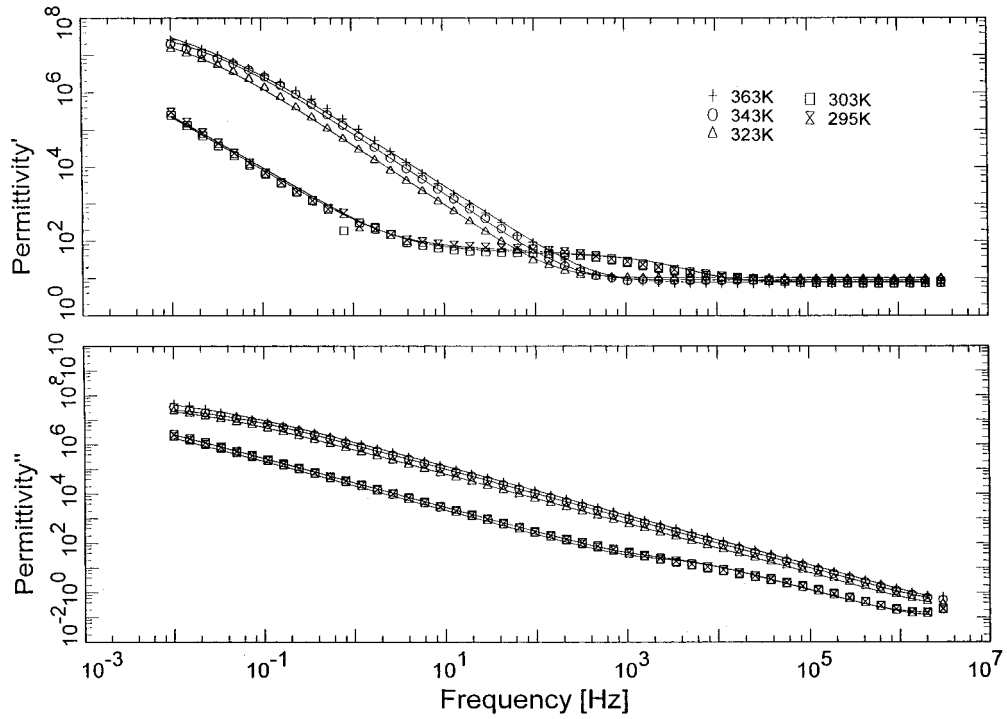

Figure 8. Fitting plots for the responses of 15% w/w water content system, showing experimental data obtained at 22, 30, 50, 70, and 90 °C. Continuous lines indicate fitted data.

has been shown to be highly sensitive to the phase behavior of the sample, particularly in terms of the resistance, which may change by up to 4 orders of magnitude on transformation from the lamellar or hexagonal phase to the cubic phase. This resistance may be associated with charge movement across the lipid bilayers. In an isotropic system such as the cubic phase, continuous charge transport routes will be present. In the lamellar or hexagonal phases, however, charge transport will inevitably become blocked due to discontinuities in the liquid crystalline structure, necessitating the movement of charge through the bilayer itself.

Overall, the study has indicated that it is possible not only to identify the different phases of liquid crystalline systems (which is often a nontrivial problem) but also to monitor discrete regions within those samples. This then carries the implication of allowing the determination of how, for example, an additional component such as a drug molecule may alter different regions within the system. Indeed, the location of such molecules within complex semisolid materials and their effect on the surrounding environment is a highly important issue, which has not yet been adequately addressed, largely due to the paucity of techniques available that are capable of providing such information. The study therefore indicates that low-frequency dielectric analysis may have a highly useful role in the structural characterization of a range of complex semisolid materials.

Acknowledgment. The authors would like to thank the EPSRC for provision of financial support for R.H. We would also like to freely acknowledge the contribution made by Dr. Pauline Geraghty (SmithKline Beecham Pharmaceuticals) and Dr. John Collett (University of Manchester) as discussions with these individuals concerning their own work led to the present study being established. Finally we would like to thank Professor Robert Hill (Kings College London, University of London) for helpful discussions and criticism of the manuscript.

References and Notes

(1) Craig, D. Q. M. *Dielectric Analysis of Pharmaceutical Systems*; Taylor and Francis; London, 1995.
(2) Jonscher, A. K. *Dielectric Relaxation in Solids*; Chelsea Dielectrics Press: London, 1983.
(3) Dissado, L. A.; Hill, R. M., *J. Chem. Soc., Faraday Trans.* **1984**, *280*, 291.
(4) Hill, R. M.; Pickup, C. *J. Mater. Sci.* **1985**, *2*, 4431.
(5) Dissado, L. A.; Rowe, R. C.; Haidar, A.; Hill, R. M. *J. Colloid Interface Sci.* **1987**, *117*, 310.
(6) Rowe, R. C.; Dissado, L. A.; Zaidi, S. H.; Hill, R. M. *J. Colloid Interface Sci.* **1988**, *122*, 354.
(7) Hill, R. M.; Cooper, J. *J. Mater. Sci.* **1993**, *28*, 1699.
(8) Hill, R. M.; Cooper, J. *J. Colloid Interface Sci.* **1995**, *174*, 24.
(9) Cooper, J.; Hill, R. M. *J. Colloid Interface Sci.* **1996**, *180*, 27.
(10) Binns, J. S.; Craig, D. Q. M.; Hill, R. M.; Davies, M. C.; Melia, C. D.; Newton, J. M. *J. Mater. Chem.* **1992**, *2*, 545.
(11) Craig, D. Q. M.; Hill, R. M.; Newton, J. M. *J. Mater. Sci.* **1993**, *28*, 1978.
(12) Craig, D. Q. M.; McDonald, C. *J. Phys. Chem.* **1995**, *99*, 5413.
(13) Tamburic, S.; Craig, D. Q. M. *J. Controlled Release* **1995**, *37*, 59.
(14) Sutananta, W.; Craig, D. Q. M.; Hill, R. M.; Newton, J. M. *Int. J. Pharm.* **1995**, *125*, 123.
(15) Larsson, K. *J. Phys. Chem.* **1989**, *93*, 7304.
(16) Engstrom, S.; Engstrom, L. *Int. J. Pharm.* **1992**, *79*, 113.
(17) Geraghty, P. B.; Attwood, D.; Collett, J. H.; Dandiker, Y. *Pharm. Res.* **1996**, *13*, 1265.
(18) Engstrom, S. *Lipid Technol.* **1990**, *2*, 42.